Bioorganic & Medicinal Chemistry Letters 24 (2014) 2066–2072

Contents lists available at ScienceDirect

Bioorganic & Medicinal Chemistry Letters

journal homepage: www.elsevier.com/locate/bmcl

Identification and optimization of indolo[2,3-*c*]quinoline inhibitors of IRAK4

L. Nathan Tumey [a,*], Diane H. Boschelli [a], Niala Bhagirath [a], Jaechul Shim [a], Elizabeth A. Murphy [b], Deborah Goodwin [b], Eric M. Bennett [c], Mengmeng Wang [d], Lih-Ling Lin [b], Barry Press [a], Marina Shen [b], Richard K. Frisbie [a], Paul Morgan [b], Shashi Mohan [b], Julia Shin [b], Vikram R. Rao [b]

[a] *Pfizer Global R&D, 445 Eastern Point Rd., Groton, CT 06340, USA*
[b] *Pfizer Global R&D, 200 Cambridge Park Dr., Cambridge, MA 02140, USA*
[c] *Pfizer Global R&D, 87 Cambridgepark Dr., Cambridge, MA 02140, USA*
[d] *Pfizer Global R&D, 1 Burtt Rd., Andover, MA 01810, USA*

ARTICLE INFO

Article history:
Received 10 February 2014
Revised 17 March 2014
Accepted 18 March 2014
Available online 29 March 2014

Keywords:
TLR signaling
Indoloquinoline
IRAK4
Kinase inhibitor
Inflammation

ABSTRACT

IRAK4 is responsible for initiating signaling from Toll-like receptors (TLRs) and members of the IL-1/18 receptor family. Kinase-inactive knock-ins and targeted deletions of IRAK4 in mice cause reductions in TLR induced pro-inflammatory cytokines and these mice are resistant to various models of arthritis. Herein we report the identification and optimization of a series of potent IRAK4 inhibitors. Representative examples from this series showed excellent selectivity over a panel of kinases, including the kinases known to play a role in TLR-mediated signaling. The compounds exhibited low nM potency in LPS- and R848-induced cytokine assays indicating that they are blocking the TLR signaling pathway. A key compound (**26**) from this series was profiled in more detail and found to have an excellent pharmaceutical profile as measured by predictive assays such as microsomal stability, TPSA, solubility, and *c*log*P*. However, this compound was found to afford poor exposure in mouse upon IP or IV administration. We found that removal of the ionizable solubilizing group (**32**) led to increased exposure, presumably due to increased permeability. Compounds **26** and **32**, when dosed to plasma levels corresponding to ex vivo whole blood potency, were shown to inhibit LPS-induced TNFα in an in vivo murine model. To our knowledge, this is the first published in vivo demonstration that inhibition of the IRAK4 pathway by a small molecule can recapitulate the phenotype of IRAK4 knockout mice.

In the past decade there has been considerable interest in targeting the innate immune system in the treatment of autoimmune diseases and sterile inflammation. Receptors of the innate immune system provide the first line of defense against bacterial and viral insults. These receptors recognize bacterial and viral products as well as pro-inflammatory cytokines and thereby initiate a signaling cascade that ultimately results in the up-regulation of inflammatory cytokines such as TNFα, IL6, and interferons. Recently it has become apparent that self-generated ligands such as nucleic acids and products of inflammation such as HMGB1 and Advanced Glycated End-products (AGE) are ligands for Toll-like receptors (TLRs) which are key receptors of the innate immune system.[1–3] This demonstrates the role of TLRs in the initiation and perpetuation of inflammation due to autoimmunity.

Interleukin-1 receptor associated kinase (IRAK4) is a ubiquitously expressed serine/threonine kinase involved in the regulation of innate immunity.[4] IRAK4 is responsible for initiating signaling from TLRs and members of the IL-1/18 receptor family. Kinase-inactive knock-ins and targeted deletions of IRAK4 in mice lead to reductions in TLR and IL-1 induced pro-inflammatory cytokines.[5–7] IRAK-4 kinase-dead knock-in mice have been shown to be resistant to induced joint inflammation in the antigen-induced-arthritis (AIA) and serum transfer-induced (K/BxN) arthritis models.[8] Likewise, humans deficient in IRAK4 also display the inability to respond to challenge by TLR ligands and IL-1.[9] However, the immunodeficient phenotype of IRAK4-null individuals is narrowly restricted to challenge by gram positive bacteria, but not gram negative bacteria, viruses or fungi. This gram positive sensitivity also lessens with age implying redundant or compensatory mechanisms for innate immunity in the absence of IRAK4.[10] *These data suggest that inhibitors of IRAK4 kinase activity will have therapeutic value in treating cytokine driven autoimmune diseases while having minimal immunosuppressive side effects.* Additional recent studies suggest that targeting IRAK4 may be a viable strategy for the treatment of other inflammatory pathologies such as atherosclerosis.[11]

* Corresponding author. Tel.: +1 860 715 6440.
E-mail address: Nathan.tumey@pfizer.com (L.N. Tumey).

http://dx.doi.org/10.1016/j.bmcl.2014.03.056
0960-894X/

Indeed, the therapeutic potential of IRAK4 inhibitors has been recognized by others within the drug-discovery community as evidenced by the variety of IRAK4 inhibitors have been reported to-date.[12–16] However, limited data has been published about these compounds and they appear to suffer from a variety of issues such as poor kinase selectivity and poor whole-blood potency that preclude their advancement into the pre-clinical models. To the best of our knowledge, no in vivo studies of IRAK4 inhibitors have been reported to-date in the literature. Herein we report a new class of IRAK4 inhibitors that are shown to recapitulate the phenotype observed in IRAK4 knockout and kinase-dead mice.

An aggressive high-throughput screening approach was undertaken in order to identify lead compounds that could be advanced quickly into a medicinal chemistry program. A Caliper high throughput screen was run using the kinase domain of IRAK4 and an in-house optimized peptide substrate. Approximately 350,000 compounds were evaluated resulting in 1935 hits that were reconfirmed in a 5-point dose–response assay and further evaluated using a DELFIA-based assay. The hits were prioritized based on factors such as potency, kinase selectivity, and synthetic tractability. These efforts led to the identification of multiple lead series that will be described in due course. One lead series that was identified contained a 3-substituted-4-aminoquinoline, as illustrated by compound **3**.

The early SAR around this series was quite erratic and difficult to interpret. For example, compound **3** initially was thought to be a 95 nM inhibitor of IRAK4. However, resynthesis of **3** resulted in a batch that was found to be nearly 1000-fold less potent. After assay variability and compound stability issues were ruled out, a closer look at the analytical data for compound **3** revealed a trace amount (~3% by UV) of a contaminant with a molecular mass consistent with indolo[2,3-*c*]quinoline **4** and/or **5**. This compound presumably arises from an intramolecular direct arylation, a reaction with significant precedent in literature.[17] We observed that the less active batch of **3** contained far smaller amounts of the impurity. Together these results strongly implied that the activity of compound **3** may be coming from the trace indolo[2,3-*c*]quinoline **4** or **5**.

A more robust synthesis of compound **4**/**5** was required in order to test the above hypothesis. The initial synthesis was accomplished by treating compound **2** under standard Suzuki conditions, but in the absence of a boronic acid coupling partner and resulted in a mixture of the regiomers **4** and **5** along with significant amounts of des-iodo **2**. The 9-cyano-indolo[2,3-*c*]quinoline **4** was purified from the mixture by reverse-phase HPLC and found to be a 7.4 nM inhibitor of IRAK4. The corresponding 7-isomer (**5**) was found to be at least 15-fold less active, although the exact IC_{50} value is questionable due to the inability to completely purify it from residual amounts **4**. The exceptional potency of compound **4** confirmed our suspicions that the observed activity of the 3-cyclopropylquinoline (**3**) was likely due to trace contamination of the sample with the isomeric cyano-indolo[2,3-*c*]quinolines **4/5**.

In order to plan and prioritize SAR studies of compound **5**, it was necessary to have some understanding of the binding mode and key interactions that this compound might make with IRAK4. Therefore, a docking study of this compound was performed using a 100,000 step MCMM/LMCS Monte Carlo procedure in MacroModel 9.6 (MMFFs and GB/SA energetics) with the published IRAK4 crystal structure complex with staurosporine.[18] The procedure found 20 binding modes within 10 kcal/mol of the global minimum, which was consistent with the SAR. Higher energy modes either did not form hydrogen bonds with the hinge or exhibited defects such as poor shape complementarity near the gatekeeper or inconsistencies with accumulated SAR. Several of the 20 modes differed from the global minimum only by minor changes to side chain rotamers for residues (197, 200, 213, 229, 233, 262, 264, 313, 329) which were unrestrained along with the inhibitor during the energy minimization. The global minimum is illustrated in Figure 1. The model strongly suggests that the quinoline nitrogen makes a key interaction with the 'hinge' methionine (Met265), in a similar manner to a variety of related quinoline and quinazoline kinase inhibitors. The cyanophenyl 'headpiece' reaches deep into the binding pocket, with the nitrile forming a hydrogen-bond with the catalytic lysine (Lys213). The 7 and 8 position of the indolo[2,3-*c*]quinoline rest snuggly against the unusually large gatekeeper residue, Tyr262. This large gatekeeper residue is unique to the IRAK family of kinases, of which only IRAK1 and IRAK4 are kinase-active proteins. Finally, the dimethoxy moiety points out toward a solvent exposed region.

With the above binding mode in mind, a series of analogs were made to probe the SAR around the cyanophenyl 'headpiece' and the quinoline core. Generally, mixtures of 7 and 9-substituted indolo[2,3-*c*]quinolines were made by taking advantage of the oxidative cyclization described above in Scheme 1. However, the yield of this synthesis was low and the separation of the two isomers proved to be quite challenging. Scheme 2 illustrates a regiospecific synthesis of 9-substituted indolo[2,3-*c*]quinolines that relies on a 2-aminoboronic acid that participates in a tandem Suzuki and intramolecular S_NAr reaction. Using these two routes, a variety of analogs (**6**–**15**) were made in order to probe the hypothesized binding mode. As predicted, the observed SAR around the tetracyclic core is consistent with the docking studies outlined above (Table 1). Movement of the cyano functionality to the 7, 8 and 10 position of the indolo[2,3-*c*]quinoline resulted in a precipitous loss of activity (compounds **5**, **6**, and **7**, respectively). This is consistent with the 7 and 8 position of molecule sitting in very close proximity to the tyrosine gatekeeper. Likewise, the addition of a methyl group to the quinoline core (**8**) resulted in a dramatic loss in activity, likely disrupting the hinge-binding interaction with Met265 due to unfavorable steric contacts between the methyl group and the backbone of residues 263–264. The incorporation of a methyl group at the analogous position in related quinazoline and quinoline-based kinase inhibitors also results in dramatic loss of activity.[19,20] A variety of functionality was incorporated in order to replace the cyano functionality on the headpiece. (**9**–**15**) Elimination of the cyano group (**15**) resulted in a 100-fold loss in activity while replacement with a nitro (**13**) or carboxamide (**12**) retained significant potency. A variety of attempts to open up the tetracyclic ring system resulted in loss of activity (**16**–**19**).

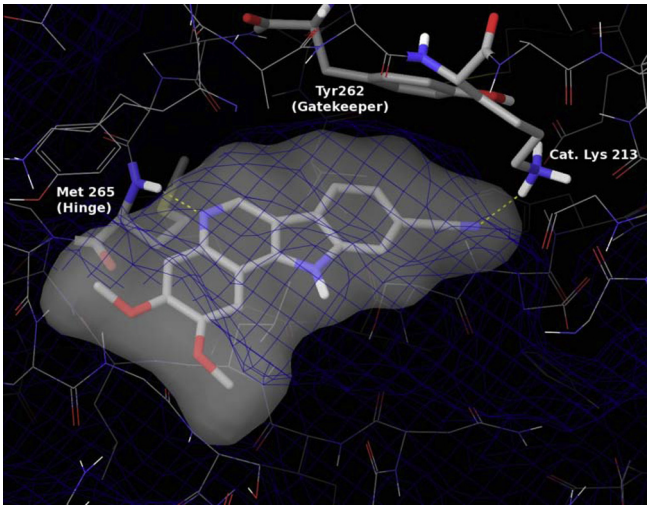

Figure 1. The proposed binding mode of compound **4** with IRAK4. The surface of the indoloquinoline is represented in grey while the protein surface is represented by the blue grid.

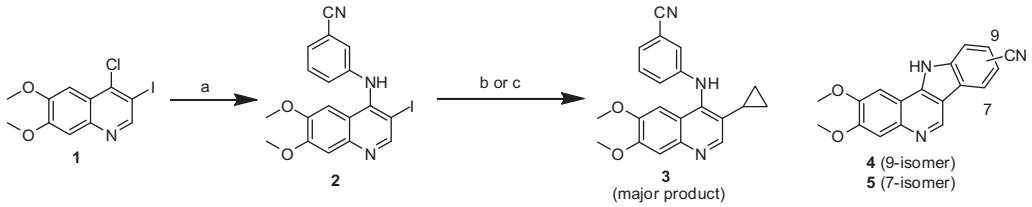

Scheme 1. Reagents and conditions: (a) 3-Amino-benzonitrile, EtOH, reflux; (b) cyclopropyl boronic acid, $Pd(PPh_3)_2Cl_2$, Cs_2CO_3, THF/H_2O, 85 °C; (c) $Pd(PPh_3)_2Cl_2$, Cs_2CO_3, THF/H_2O, 85 °C.

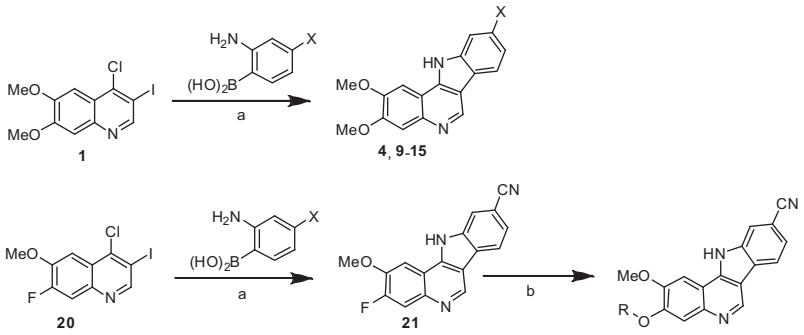

Scheme 2. Reagents and conditions: (a) $Pd(PPh_3)_4$, Cs_2CO_3, 3:1 DME/H_2O, 100 °C,16 h; (b) ROH, NaH (4 equiv), DMF, 110 °C, 16 h.

Table 1
SAR around the cyanophenyl 'headpiece'

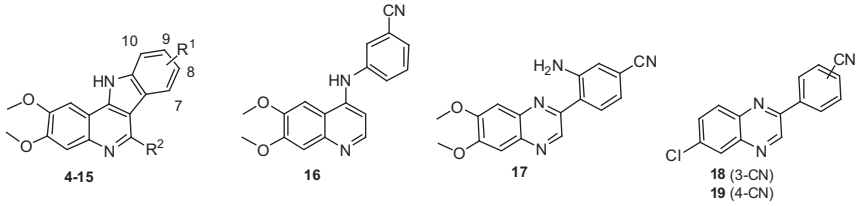

Compd#	R^1	R^2	IRAK4 IC_{50} (nM)
4	9-CN	H	7.4
5	7-CN	H	130[#]
6	8-CN	H	30,000
7	10-CN	H	5100
8	9/7-CN	Me	14,000[§]
9	9-CF_3	H	92
10	9-OMe	H	615
11	9-OCF_3	H	2480
12	9-$CONH_2$	H	26
13	9-NO_2	H	5.3
14	9-NHAc	H	23,600
15	H	H	630
16	NA		19,000
17	NA		>100,000
18	NA		>100,000
19	NA		>100,000

[#] Compound **5** was contaminated with ~5% of compound **4**. It is believed (though unconfirmed) that the observed activity of compound **5** is due entirely to this contamination.
[§] Compound **8** was made as an inseparable mixture of the 9 and 7 isomers.

Despite its excellent potency in biochemical assays, it was quite apparent that compound **4** would not be suitable for in vivo studies due largely to its exceptionally poor solubility. Attempts to improve the solubility by breaking up the tetracyclic core failed to give compounds with meaningful inhibition of IRAK4 (**16**–**19**, above). Therefore, we next turned our attention to the addition of polar tailpieces that would point into the solvent exposed area of the binding pocket. Modeling studies (above) suggested that the 3-methoxy group is oriented in a favorable direction to reach into bulk solvent. With this in mind, a series of analogs was prepared that incorporated amine and ether containing tailpieces. (**22**–**32**) The synthesis of these analogs is outlined in Scheme 2 and generally relied on an S_NAr reaction of an alkoxide with 3-fluoroindolo[2,3-*c*]quinoline **21**. To our delight, the addition of solubilizing tailpieces generally resulted in a further boost in potency, yielding sub-nM inhibitors of IRAK4 (Table 2). The 3-carbon tail generally provided additional potency as compared to the 2-carbon tails, as observed by comparing **22** and **24** to their longer-chain counterparts, **23** and **26**. All compounds with the amine-containing tails (**22**–**29**) were observed to have excellent solubility (generally

Table 2
SAR around the solubilizing tailpiece

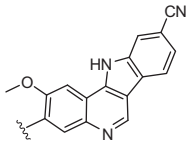

Compd#	Structure	IRAK4 IC_{50} (nM)	IRAK1 IC_{50} (nM)	hPBMC R848 induced TNFα (nM)	hWB R848-induced IL6 (nM)	Solubility (pH 7.4)
4	MeO–	7.4	NA	NA	NA	0 μg/mL
22	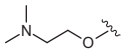	2.6	120	41	2700	>100 μg/mL
23	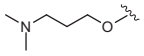	0.29	130	24	4300	>100 μg/mL
24	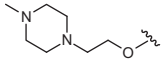	0.75	170	9.8	850	>100 μg/mL
25	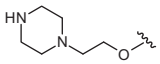	2.6	120	134	14,000	69 μg/mL
26	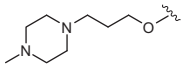	0.094	65	85	950	>100 μg/mL
27	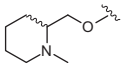	0.10	68	44	1400	68 μg/mL
28	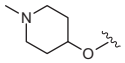	6.2	310	890	2700	68 μg/mL
29	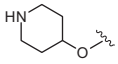	6.3	310	1800	>10,000	71 μg/mL
29	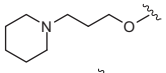	0.11	86	200	960	>100
30	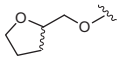	0.46	210	36	3600	0 μg/mL
31	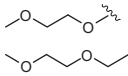	0.55	260		4700	0 μg/mL
32	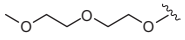	1.3	290	18	8300	0 μg/mL

>70 μg/mL) while those with ether-containing tails (**30**–**32**) were found to have poor solubility.

Having now established excellent enzymatic potency against IRAK4, we next turned our attention to the functional activity of this novel class of inhibitor. Compounds of interest were screened for their ability to inhibit R848 induced TNF in primary human monocytes (hPBMCs).[21] R848 activation of TLR7 and TLR8 on monocytes results in the production of pro-inflammatory cytokines such as IL-6 and TNFα. The compounds shown in Table 2 were screened in this cellular assay and found to potently inhibit this activity. Compounds were generally 10 to 100-fold less potent in the cellular assay as compared to the enzymatic assay, possibly indicating a permeability or efflux issue (vide infra). Compounds containing secondary amines (e.g., **25**) were found to be very weakly active in the cellular assay, presumably due to poor permeability.

Additionally, compounds were screened for their ability to block R848-induced release of IL6 in human whole blood (hWB). As can be seen in Table 2, the most potent compounds in the hPBMC assay were found to have low micromolar activity in human whole blood. The discrepancy between the cellular and whole-blood potencies is most likely attributable to plasma protein binding, which is >99% for two compounds tested (see Table 4 and related discussion).

A key hurdle in all kinase drug-discovery programs is the establishment of appropriate levels of selectivity over off-target enzymes that may lead to toxicity. Additionally, most signaling cascades consist of numerous kinases and the inhibition of multiple pathway kinases can complicate the interpretation of results from functional assays and efficacy studies. One persistent issue in the development of IRAK4 inhibitors is the importance of the contribution of activity of IRAK1 to the cellular potency of the compounds. Several studies have postulated that inhibition of IRAK4 and IRAK1 may be required for the inhibition of proinflammatory cytokines.[22] Therefore we strove for selectivity over the related isoform, IRAK1, in order to determine whether dual inhibition of both isoforms would be necessary for blockage of the TLR pathway (Table 2). Encouragingly, most compounds showed >100-fold selectivity over this kinase. Both IRAK1 and IRAK4 inhibition were evaluated in the presence of ATP at their K_m (35 μM and 600 μM, respectively).[31] The tighter binding of IRAK1 to ATP suggests that the high levels of cellular ATP (1–2 mM) will limit the functional potency of these inhibitors against IRAK1 even more than the IC_{50} values in Table 2 suggest. Therefore, it can be inferred that most of the cellular and hWB activity described in Table 2 is derived from the inhibition of IRAK4.

Compounds of key interest were additionally evaluated against a panel of kinases selected based on sequence diversity and safety concerns. The summarized data is shown in Table 3. All kinases (including IRAK4) were tested with the ATP concentration at the K_m. The desired selectivity profile for drug discovery programs varies greatly depending upon the indication being pursued and the stage of the program. While there is great debate in the field about the desirable selectivity profile for oncology applications,[23] it is relatively well-agreed that pursuit of a non-oncology indication requires very stringent criteria for compound advancement. Our

Table 3
Kinase selectivity for selected IRAK4 inhibitors (shown as fold-selectivity compared to the IRAK4 IC_{50} in Table 2)

	4	22	23	26	27	28	31
Itk	30	52	130	490	280	90	
PI3Kα	230		>25000				
PI3Kγ	460		>25000				
LCK	330	35	180	640	750	140	
ABL	110	45	140	390	880	250	630
Aurora B	11	87	360	370	1200	120	75
CDK1	6	51	680	210	1600	72	52
CDK2	81	390	15000	5100	11000	920	2200
CHK1	14	9	20	120	100	12	67
CK1γ	>12000	>19000	>125000	>500000	>500000	>8100	>83000
ERK2	>12000	>19000	>125000	>500000	>500000	6100	>83000
FGFR1							>83000
FYN	160	99	510	570	970	1400	
GCK	75	65	240	480	2600	130	
GSK3α							>83000
GSK3β							>83000
HCK	200	990		1800	5500	5400	
IKKα			98000				13000
JNK1			1800				
LYN A	84	150	670	1100	2500	>16000	
MET	>12000					3700	>83000
MK2	>12000	18000	100000	190000			15000
P38α	>12000	>19000	>125000	>500000	>500000	1100	>83000
PDGFRα	1	2	13	50	50	>8100	8
PKA	>12000	>19000	>125000	>500000	>500000	2	>83000
PKBα		>19000	>125000	>500000	>500000	4199	>83000
PKCα	>12000	8000	32000	120000	93000		

primary goal at this stage of the program, however, was to achieve proof-of-mechanism in vivo in order to justify continued investment. With this in mind, the selectivity for most of the compounds shown in Table 2 was thought to be adequate. Indeed, the selectivity ratios for the vast majority of the kinases tested were >>100-fold. Most compounds showed poor selectivity against only three kinases: CHK1, PDGFRα, and VEGFR2. The selectivity of these compounds is fascinating in light of the fact that the proposed key interactions with the hinge (Met265) and the catalytic lysine (Lys213) should be common to nearly all kinases. We believe that the observed selectivity for this class of compounds partially arises from the tight association of the 'southern' face of the indolo[2,3-*c*]quinoline with the gatekeeper (Tyr262). Tyrosine gatekeepers are unique to the IRAK family of kinases, of which only IRAK-1 and IRAK-4 are kinase-active. Only approximately 15% of kinases have aromatic gatekeepers, and the vast majority of these are phenylalanine.[24] The relative rarity of aromatic gatekeepers combined with the very tight SAR around the 'gatekeeper' region of the core lead us to believe that this interaction may play an key role in the observed selectivity.

While the modest off-target activity (particularly against VEGFR2 and PDGFR) was certainly a concern, it was gratifying to see that the compounds in Table 3 possessed minimal activity against kinases involved in the TLR-signaling pathway, namely LCK, P38α, and MK2.[25] This gave us increased confidence that the inhibition of R848-induced cytokine activity (Table 2) could, in fact, be attributed to IRAK4 inhibition. Armed with this information, the compounds were examined in further depth to identify one or more that could be advanced into in vivo proof-of-concept studies to show that IRAK4 inhibition can block TLR signaling in an animal model.

Table 4
Pharmaceutical profile of two advanced leads

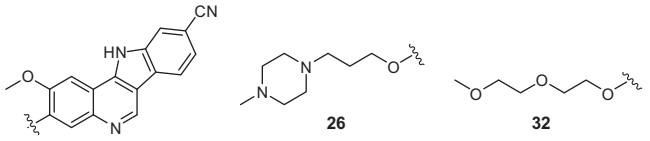

26 **32**

hIRAK4 IC_{50}	0.094 nM	1.3 nM
hPBMC R848 induced IL6 IC_{50}	85 nM	18 nM
THP cell LPS-induced TNFα IC_{50}	56 nM	29 nM
hWB R848 induced IL6 IC_{50}	950 nM	8300 nM
hWB LPS induced TNFα IC_{50}	5500 nM	15,000 nM
MW	430	390
*c*log*P*	3.2	3.5
TPSA	77 Å^2	89 Å^2
Microsomal stability ($t_{1/2}$)		
Rat	>30 min	23 min
Mouse	>30 min	10 min
Human	>30 min	20 min
Cyp,% inhibition @3 μM		
2C9	11%	11%
2D6	0%	8%
3A4	15%	−7%
Human plasma binding (% free)	0.8%	0.9%
MDCK permeability		
A to B (cm/s)	0.10×10^{-6}	0.6×10^{-6}
Efflux ratio	78	71
10 mpk mouse PK (IP)		
AUC (h ng/mL)	540	6500
C_{max} (μM)	0.75	5.5
100 mpk mouse PK (IP)		
AUC (h ng/mL)	10,000	NA
C_{max} (μM)	14	NA
2 mpk mouse PK (IV)		
Cl (mL/min kg)	37	29
V_d (L/kg)	34	1.2
AUC (h ng/mL)	900	580
10 mpk mouse PK (PO)		
AUC (h ng/mL)	80	650
%*F*	2%	11%

Compounds of interest were routinely screened for microsome stability and CYP inhibition. Indolo[2,3-*c*]quinolines with amine tails (such as **26**) generally showed excellent microsome stability across 3 species and showed minimal inhibition of Cyp2C9, 2D6, and 3A4 (Table 4). However, this compound exhibited unexpectedly poor exposure in BALB/c mice by IP or PO administration. Permeability for this compound was quite poor, as measured by A to B flux across MDR1-transfected Madine-Darby canine kidney (MDCK) monolayer. Moreover, the efflux ratio was high, strongly suggesting that this compound is a substrate for PGP.[26] (Any ratio >2 is suggestive of PGP efflux.) Since both IP and PO dosing are subject to 'first pass' metabolism in the liver, we speculated that the poor exposure may be due to either rapid metabolism or to PGP-mediated biliary excretion. However, compound **26** and related compounds (such as **23**) had excellent microsomal stability suggesting that metabolism was not a major route of elimination. Moreover, compound **23** was evaluated in a hepatocyte stability assay and found to be exceptionally stable (Cl_{int} = 0.1–0.3 μL/min/10^6 cells), only showing two minor metabolites: Demethylation and oxidation of the tertiary amine. Based on this evidence, we reasoned that the poor PK exposure of **26** must be due to PGP-mediated biliary excretion. This immediately led to two potential strategies for improved exposure. First, by 'swamping' the PGP pumps, the exposure may be improved in a non-linear manner. (In other words, the PGP pumps have a finite capacity for efflux. Once that capacity is reached, additional compound will be free to enter circulation.) Secondly, the exposure may be improved by finding a compound with a decreased efflux ratio or increased permeability.

The strategy of swamping the PGP pumps in order to increase exposure was employed successfully. Increasing the IP dose of compound **26** by 10-fold (100 mpk) increased the exposure and the C_{max} by approximately 20-fold, strongly indicating that our strategy of swamping the PGP pumps had been successful (Table 4). The measured blood levels of **26** (C_{max} = 14 μM) were now found to be in excess of the whole blood IC_{50} (5.5 μM) for approximately 3 h following the initial dose, paving the way for an in vivo proof-of-mechanism study. (vide infra).

It has been noted that PGP substrates are disproportionately hydrophobic and amphipathic, frequently containing aromatic moieties linked to strong H-bond acceptors and positively charged residues.[27,28] We therefore hypothesized that by reducing the polarity and H-bonding ability of the flexible 'tail' we may be able to reduce the affinity of the compounds towards PGP. Moreover, a non-ionized tailpiece may improve the permeability of the compound thereby decreasing the efflux ratio. Therefore, in order to find inhibitors with a decreased efflux ratio and improved permeability, a subset of the previously described compounds was tested for MDCK permeability (**22**–**33**, Table 5). As expected, compounds with tertiary amines, such as **26**–**29** were found to have very poor permeability (A–B) and high efflux ratios. Perhaps not surprisingly, the least permeable compounds (**26** and **29**) also displayed the poorest exposure upon IP administration. Ether -based solubilizing tails afforded improved permeability (A–B) but only marginally improved the efflux ratio. Interestingly, IP exposure seems to be correlated reasonably well with permeability but not with efflux ratio. This suggests that improvement in permeability can overcome some PGP liabilities. Compound **32**, with a di-ethylene glycol tail, was found to provide the best balance of plasma exposure and whole blood potency. This compound was profiled in more detail, as outlined in Table 4.

Interestingly, compound **32** was observed to be slightly more potent than compound **26** in the cellular assays (PBMCs and THPs) in spite of being approximately 10-fold less potent against IRAK4. This is consistent with its improved permeability (0.60×10^{-6} cm/s vs 0.10×10^{-6} cm/s). The improved permeability is also, presumably, largely responsible for the increased IP and PO exposure of compound **32** compared to compound **26**. This improved exposure is in spite of poorer microsomal stability (10–23 min) and increased polar surface area. Like compound **26**, compound **32** is highly protein-bound (>99%) thereby accounting for the discrepancy between the cellular potency (29 nM) and the whole-blood potency (15 μM). As mentioned previously, a 10 mg/kg dose (IP) of compound **32** resulted in approximately 10-fold higher exposure as compared to the same dose of compound **26** (536 h ng/mL vs 6500 h ng/mL). Unfortunately, the blood levels at C_{max} (5.5 μM) were still below the targeted blood levels based on the whole-blood potency (15 μM). However, based on the experience with compound **26**, we had confidence that increased doses of **32** should result in a proportional (or even super-proportional) increase in exposure. Therefore, this compound (dosed at 30 mpk by IP) was selected for advancement into an in vivo proof-of-mechanism study.

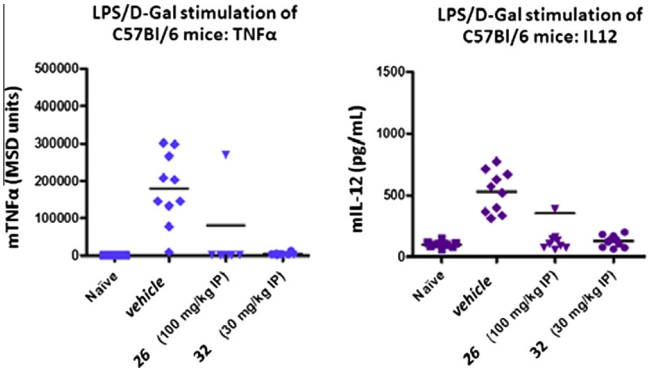

Figure 2. Stimulation of female C57Bl/6 mice with 8 mg of D-galactosamine (D-Gal) followed by 500 ng of LPS.

The proof-of-mechanism study was performed on female C57Bl/6 mice stimulated with 8 mg of D-galactosamine (D-Gal) followed by 500 ng of LPS (Fig. 2). Animals were treated with test compound or vehicle 2 h prior to stimulation with LPS. The animals were harvested 1.5 h after stimulation and the blood levels of a variety of cytokines were measured (Fig. 2). Vehicle-treated animals stimulated with LPS/D-Gal had a robust cytokine response as indicated by levels of TNFα and IL-12. However, animals treated with compound **26** (100 mpk) and compound **32** (30 mpk) showed very low circulating cytokine levels, essentially equal to naïve (non-stimulated) animals. The C_{max} unbound concentration of **26** and **32** at the administered doses are estimated to be 110 and 49 nM, respectively (based on the plasma protein binding in Table 4). These values are below the concentration necessary for inhibition of most of the kinases described in Table 3 but above the cellular IC_{50} reported in Table 2. These results strongly suggest that these compounds are blocking the TLR signaling cascade in vivo through an IRAK4 dependent mechanism.

LPS signals through the TLR-4 pathway, a signaling cascade that has been shown by numerous studies to be dependent upon IRAK4 kinase activity. Mice deficient in functional IRAK4 have been

Table 5
Permeability and AUC for selected compounds

Compd#	R	MDCK, A–B (cm/s)	MDCK efflux ratio	Mouse 10 mpk IP AUC (h ng/mL)
29	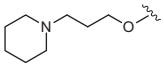	0.06×10^{-6}	216	1167
26	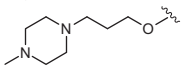	0.10×10^{-6}	78	1364
27	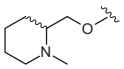	0.13×10^{-6}	263	2680
28	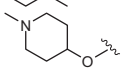	0.14×10^{-6}	167	
30	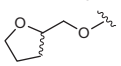	0.8×10^{-6}	40	2877
31	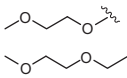	0.68×10^{-6}	45	2912
32	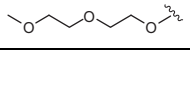	0.60×10^{-6}	73	6506

shown to have an attenuated response to LPS stimulation, showing dramatically lower levels of IL-6, IL-12, and TNFα than their wild-type counterparts.[5,29] The two inhibitors described above (**32** and **26**) were shown to essentially recapitulate this phenotype in non-mutant mice. Therefore, it is hoped that the resistance to joint-inflammation that has been reported for IRAK4 deficient mice will also be observed for these compounds.[8] Moreover, based on several recently reported studies of IRAK4-deficient patients, we believe that the actions exhibited by these compounds may translate into human efficacy. Whole blood and PBMCs isolated from IRAK4-deficient patents have been shown to be nonresponsive to LPS stimulation and other TLR-ligands (except for TLR3 ligands).[10,30] Therefore, we are optimistic that blockage of IRAK4 signaling by inhibitors such as those described in this Letter will ultimately be therapeutically useful in human disease.

Acknowledgments

We would like to thank Katherine Lee for advice and useful discussion during the project and during drafting of this report. We also thank Mala Gopalsamy and the exploratory chemistry team for identifying this lead series. We are greatful to the members of the Wyeth Chemical Technologies (CT) and Drug-Safety and Metabolism (DSM) team for performing the pharmaceutical profiling. Finally, we would also like to thank Li Di for helpful discussions and advice about pharmaceutical properties and PK results.

Supplementary data

Supplementary data associated with this article can be found, in the online version, at http://dx.doi.org/10.1016/j.bmcl.2014.03.056.

References and notes

1. O'Neill, L. A. J. *Curr. Opin. Pharmacol.* **2003**, *3*, 396.
2. Kanzler, H.; Barrat, F. J.; Hessel, E. M.; Coffman, R. L. *Nat. Med.* **2007**, *13*, 552.
3. Wagner, H. *Adv. Immunol.* **2006**, *91*, 159.
4. Suzuki, N.; Saito, T. *Trends Immunol.* **2006**, *27*, 566.
5. Kawagoe, T.; Sato, S.; Jung, A.; Yamamoto, M.; Matsui, K.; Kato, H.; Uematsu, S.; Takeuchi, O.; Akira, S. *J. Exp. Med.* **2007**, *204*, 1013.
6. Fraczek, J.; Kim, T. W.; Xiao, H.; Yao, J.; Wen, Q.; Li, Y.; Casanova, J.-L.; Pryjma, J.; Li, X. *J. Biol. Chem.* **2008**, *283*, 31697.
7. Kim, T. W.; Staschke, K.; Bulek, K.; Yao, J.; Peters, K.; Oh, K.-H.; Vandenburg, Y.; Xiao, H.; Qian, W.; Hamilton, T.; Min, B.; Sen, G.; Gilmour, R.; Li, X. *J. Exp. Med.* **2007**, *204*, 1025.
8. Koziczak-Holbro, M.; Littlewood-Evans, A.; Pollinger, B.; Kovarik, J.; Dawson, J.; Zenke, G.; Burkhart, C.; Muller, M.; Gram, H. *Arthritis Rheum.* **2009**, *60*, 1661.
9. Hernandez, M.; Bastian, J. F. *Curr. Allergy Asthma Rep.* **2006**, *6*, 468.
10. Lavine, E.; Somech, R.; Zhang, J. Y.; Puel, A.; Bossuyt, X.; Picard, C.; Casanova, J. L.; Roifman, C. M. *J. Allergy Clin. Immunol.* **2007**, *120*, 948.
11. Rekhter, M.; Staschke, K.; Estridge, T.; Rutherford, P.; Jackson, N.; Gifford-Moore, D.; Foxworthy, P.; Reidy, C.; Huang, X.-d.; Kalbfleisch, M.; Hui, K.; Kuo, M.-S.; Gilmour, R.; Vlahos, C. *J. Biochem. Biophys. Res. Commun.* **2008**, *367*, 642.
12. Wang, Z.; Wesche, H.; Stevens, T.; Walker, N.; Yeh, W.-C. *Curr. Top. Med. Chem.* **2009**, *9*, 724.
13. Buckley, G. M.; Fosbeary, R.; Fraser, J. L.; Gowers, L.; Higueruelo, A. P.; James, L. A.; Jenkins, K.; Mack, S. R.; Morgan, T.; Parry, D. M.; Pitt, W. R.; Rausch, O.; Richard, M. D.; Sabin, V. *Bioorg. Med. Chem. Lett.* **2008**, *18*, 3656.
14. Buckley, G. M.; Ceska, T. A.; Fraser, J. L.; Gowers, L.; Groom, C. R.; Higueruelo, A. P.; Jenkins, K.; Mack, S. R.; Morgan, T.; Parry, D. M.; Pitt, W. R.; Rausch, O.; Richard, M. D.; Sabin, V. *Bioorg. Med. Chem. Lett.* **2008**, *18*, 3291.
15. Buckley, G. M.; Gowers, L.; Higueruelo, A. P.; Jenkins, K.; Mack, S. R.; Morgan, T.; Parry, D. M.; Pitt, W. R.; Rausch, O.; Richard, M. D.; Sabin, V.; Fraser, J. L. *Bioorg. Med. Chem. Lett.* **2008**, *18*, 3211.
16. Powers, J. P.; Li, S.; Jaen, J. C.; Liu, J.; Walker, N. P. C.; Wang, Z.; Wesche, H. *Bioorg. Med. Chem. Lett.* **2006**, *16*, 2842.
17. Campeau, L.-C.; Parisien, M.; Jean, A.; Fagnou, K. *J. Am. Chem. Soc.* **2006**, *128*, 581.
18. Wang, Z.; Liu, J.; Sudom, A.; Ayres, M.; Li, S.; Wesche, H.; Powers, J. P.; Walker, N. P. C. *Structure* **2006**, *14*, 1835.
19. Hu, Y.; Green, N.; Gavrin, L. K.; Janz, K.; Kaila, N.; Li, H.-Q.; Thomason, J. R.; Cuozzo, J. W.; Hall, J. P.; Hsu, S.; Nickerson-Nutter, C.; Telliez, J.-B.; Lin, L.-L.; Tam, S. *Bioorg. Med. Chem. Lett.* **2006**, *16*, 6067.
20. Bridges, A. J.; Zhou, H.; Cody, D. R.; Rewcastle, G. W.; McMichael, A.; Showalter, H. D. H.; Fry, D. W.; Kraker, A. J.; Denny, W. A. *J. Med. Chem.* **1996**, *39*, 267.
21. Gorden, K. B.; Gorski, K. S.; Gibson, S. J.; Kedl, R. M.; Kieper, W. C.; Qiu, X.; Tomai, M. A.; Alkan, S. S.; Vasilakos, J. P. *J. Immunol.* **2005**, *174*, 1259.
22. Qin, J.; Jiang, Z.; Qian, Y.; Casanova, J.-L.; Li, X. *J. Biol. Chem.* **2004**, *279*, 26748.
23. Morphy, R. *J. Med. Chem.* **2010**, *53*, 1413–1437.
24. Zuccotto, F.; Ardini, E.; Casale, E.; Angiolini, M. *J. Med. Chem.* **2010**, *53*, 2681.
25. Gaestel, M.; Kotlyarov, A.; Kracht, M. *Nat. Rev. Drug Disc.* **2009**, *8*, 480.
26. del Amo Eva, M.; Heikkinen Aki, T.; Monkkonen, J. *Eur. J. Pharm. Sci.* **2009**, *36*, 200.
27. Penzotti, J. E.; Lamb, M. L.; Evensen, E.; Grootenhuis, P. D. J. *J. Med. Chem.* **2002**, *45*, 1737.
28. Eckford, P. D. W.; Sharom, F. J. *Chem. Rev.* **2009**, *109*, 2989.
29. Koziczak-Holbro, M.; Gluck, A.; Tschopp, C.; Mathison, J. C.; Gram, H. *Eur. J. Immunol.* **2008**, *38*, 788.
30. Ku, C.-L.; von Bernuth, H.; Picard, C.; Zhang, S.-Y.; Chang, H.-H.; Yang, K.; Chrabieh, M.; Issekutz, A. C.; Cunningham, C. K.; Gallin, J.; Holland, S. M.; Roifman, C.; Ehl, S.; Smart, J.; Tang, M.; Barrat, F. J.; Levy, O.; McDonald, D.; Day-Good, N. K.; Miller, R.; Takada, H.; Hara, T.; Al-Hajjar, S.; Al-Ghonaium, A.; Speert, D.; Sanlaville, D.; Li, X.; Geissmann, F.; Vivier, E.; Marodi, L.; Garty, B.-Z.; Chapel, H.; Rodriguez-Gallego, C.; Bossuyt, X.; Abel, L.; Puel, A.; Casanova, J.-L. *J. Exp. Med.* **2007**, *204*, 2407.
31. Cushing, L.; Stochaj, W.; Siegel, M.; Czerwinski, R.; Dower, K.; Wright, Q.; Hirschfield, M.; Casanova, J.L.; Picard, C.; Puel, A.; Lin, L.L.; Rao, V. *J. Biol. Chem.* **2014**, in press.